Synthesis and Structure of Carbonyl−Metalated Organobismuth Complexes

Robert E. Bachman and Kenton H. Whitmire*

Department of Chemistry, Rice University, P.O. Box 1892, Houston, Texas 77251

Received June 14, 1994[⊗]

The reaction of Ph_2BiCl with the dinuclear group VI anions $[M_2(CO)_{10}]^{2-}$ (M = Cr, Mo, W) produces the isostructrual mixed organo−metal complexes $[Ph_2Bi\{M(CO)_5\}_2]^-$ ([**1a**]$^-$, M = Cr; [**1b**]$^-$, M = Mo; [**1c**]$^-$, M = W). The $[PPN]^+$ salts of these three clusters were characterized both spectroscopically and structurally. [PPN][**1a**] crystallizes in the triclinic space group $P\bar{1}$ (No. 2) with cell constants a = 12.622(6) Å, b = 12.800(6) Å, c = 16.798(6) Å, α = 84.05(3)°, β = 87.89(3)°, γ = 88.86(3)°, and V = 2697.3(3.7) Å^3. [PPN][**1b**] crystallizes in an isomorphous unit cell with a = 12.738(4) Å, b = 12.967(3) Å, c = 16.817(7) Å, α = 84.60(3)°, β = 87.95(3)°, γ = 88.38(3)°, and V = 2762.9(3.0) Å^3. [PPN][**1c**] crystallizes as a combination toluene/ether solvate in the monoclinic space group $P2_1/n$ (No. 14) with unit cell constants a = 9.833(5) Å, b = 28.166(10) Å, c = 24.037(14) Å, β = 94.79(5)°, and V = 6634.3(5.7) Å^3. The analogous reaction of Ph_2BiCl with $[Fe_2(CO)_8]^{2-}$ yields $[Ph_2Bi\{Fe(CO)_4\}_2]^-$ ([**2**]$^-$). This complex can also be prepared from the reaction of the previously reported $[Ph_2BiFe(CO)_4]^-$ with $Fe_2(CO)_9$. Similarly, the reaction of $[Ph_2BiFe(CO)_4]^-$ with $Cr(CO)_5THF$ generates the heterometallic cluster $[Ph_2Bi\{Fe(CO)_4\}\{Cr(CO)_5\}]^-$ ([**3**]$^-$). [Et_4N][**2**] crystallizes in the monoclinic space group $P2_1/n$ (No. 14) with cell constants a = 13.064(3) Å, b = 14.309(3) Å, c = 16.951(3) Å, β = 100.21(3)°, and V = 3118.5(1.1) Å^3. [PPN][**3**] crystallizes as an ether solvate in the space group $P\bar{1}$ (No. 2) with cell constants a = 10.998(2) Å, b = 16.244(3) Å, c = 17.203(3) Å, α = 85.60(3)°, β = 76.42(3)°, γ = 80.13(3)°, and V = 2941.1(9) Å^3. Comparison of the structural parameters in these and other related complexes indicates that the hybridization of the bismuth atom is dependent on its coordination environment. Initial attempts at producing higher nuclearity clusters through controlled oxidations have led to complete degradation of the complexes and production of simple metal carbonyl compounds such as $Cr(CO)_5(MeCN)$. In this case, the identity of the carbonyl compound was confirmed crystallographically. $Cr(CO)_5(MeCN)$ crystallizes in the space group $P\bar{1}$ (No. 2) with unit cell constants a = 6.2140(10) Å, b = 12.167(2) Å, c = 13.402(3) Å, α = 85.38(3)°, β = 86.84(3)°, γ = 86.30(3)°, V = 1006.6(3) Å^3, and Z = 4.

Introduction

Organobismuth compounds have been investigated extensively for many years.[1] However, much less is known about organobismuth species which also incorporate transition metal fragments.[2] Complexes in which a trialkyl- or triarylbismuth fragment acts as an electron-pair donor to an unsaturated transition metal fragment make up the largest group of known organobismuth−transition metal compounds. Examples of this type include $M(CO)_5(BiR_3)$ where M = Cr, Mo, W and R = Me,[3] Et,[3,4] cyclohexyl,[3] Ph,[5] *t*-Bu,[6] as well as the disubstituted complex *cis*-$Mo(CO)_4(BiEt_3)_2$.[4] Similar results have been obtained for nickel and vanadium carbonyl species via CO substitution reactions.[4,6,7] More recently progress has been made in the synthesis of complexes which contain organobismuth fragments with less than three organic moieties bound to bismuth. In these complexes the bismuth center usually retains a lone pair and the bismuth−metal bond is most appropriately described as a covalent interaction rather than as a dative one. Examples in which the bismuth complex retains two organic fragments include $Ph_2BiMn(CO)_5$,[8] $Ph_2BiCo(CO)_3(PPh_3)$,[9] $[Ph_2BiFe(CO)_4]^-$,[8] $(Ph_2Bi)_2Fe(CO)_4$,[8] $Ph_2BiRe(CO)_5$,[10] and $Me_2BiFeCp(CO)_2$.[11] Several complexes are also known in which the bismuth is bound to only one organic moeity, such as $MeBi\{CpFe(CO)_2\}_2$,[11] $EtBi\{CpMo(CO)_3\}_2$,[12] and $PhBi\{ML_n\}_2$, with ML_n = $CpMo(CO)_3$ and $Co(CO)_3(PPh_3)$.[12] Cyclic ring complexes such as $[RBiFe(CO)_4]_2$, with R = Me[13] and Ph,[8] and the novel cluster $[W_2(CO)_8(\mu\text{-}\eta^2\text{-}Bi_2)(\mu\text{-}BiMeW(CO)_5]$ have also been reported.[14] With only a few exceptions, in all the complexes known to date, the bismuth atom is only three-coordinate and therefore retains a lone pair. This observation, combined with initial reactivity studies performed on $[Ph_2BiFe(CO)_4]^-$, suggests that this lone pair is relatively unavailable for dative bond formation.[8]

This paper explores the synthesis and reactivity of these hybrid organo−metal bismuth compounds. Particular emphasis is given to determining the generality of the synthetic methods used, the reactivity of the lone pair on bismuth (when it is present), and the effect of the coordination at bismuth on its electronic state. The complexes reported here belong to a rare class of *anionic* metalated organobismuth complexes.

[⊗] Abstract published in *Advance ACS Abstracts,* February 15, 1995.

(1) Freedman, L. D.; Doak, G. O. *Chem. Rev.* **1982**, *82*, 15.
(2) (a) Dimaio, A.-J.; Rheingold, A. L. *Chem. Rev.* **1990**, *90*, 169. (b) Scherer, O. J. *Angew. Chem.* **1990**, *102*, 1137. (c) Huttner, G.; Evertz, K. *Acc. Chem. Res.* **1986**, *19*, 406. (d) Whitmire, K. H. *Coord. Chem. B* **1988**, *17*, 95.
(3) Fischer, E. O.; Richter, K. *Chem. Ber.* **1976**, *109*, 1140.
(4) Benlian, D.; Bigorgne, M. *Bull. Soc. Chim. Fr.* **1963**, 1583.
(5) Carty, A. J.; Taylor, N. J.; Coleman, A. W.; Lappert, M. F. *J. Chem. Soc., Chem. Commun.* **1979**, 639.
(6) Schumann, H.; Breunig, H. J. *J. Organomet. Chem.* **1975**, *87*, 83.
(7) Talay, R.; Rehder, D. *Chem. Ber.* **1978**, *111*, 1978.
(8) Cassidy, J. M.; Whitmire, K. H. *Inorg. Chem.* **1991**, *30*, 2788.
(9) Calderazzo, F.; Poli, R.; Pelizzi, G. J. *J. Chem. Soc., Dalton Trans.* **1984**, 2535.
(10) Nesmeyanov, A. N.; Anisimov. K. N.; Kolbova, N. E.; Khandozhko, V. N. *Dokl. Akad. Nauk SSSR* **1969**, *156*, 383.
(11) Kaul, H.; Greissinger, D.; Luksza, M; Malisch, W. *J. Organomet. Chem.* **1982**, *228*, C29.
(12) Clegg, W.; Compton, N. A.; Errington , R. J.; Fisher, G. A.; Norman, N. C.; Wishart, N. *J. Organomet. Chem.* **1990**, *399*, C21.
(13) Whitmire, K. H.; Shieh, M.; Cassidy, J. M. *Inorg. Chem.* **1989**, *28*, 3164.
(14) Arif, A. M.; Cowley, A. H.; Norman, N. C.; Pakulski, M. *Inorg. Chem.* **1986**, *25*, 4836.

0020-1669/95/1334-1542$09.00/0

Syntheses

General Considerations. All manipulations were performed with oven-dried Schlenkware using standard techniques on a Schlenk line or in a Vacuum Atmospheres drybox.[15] All solvents were distilled from the appropriate drying agent under nitrogen prior to use: methanol (Mg); THF and ether (Na/Ph_2CO); toluene and hexanes ($LiAlH_4$); dichloromethane and acetonitrile (CaH_2). Bis(triphenylphosphine)-nitrogen(1+) chloride, [PPN]Cl,[16] Ph_2BiCl,[17] $[Et_4N]_2[Fe_2(CO)_8]$,[18] $Na_2[Fe(CO)_4]$[19] and KC_8[20] were prepared according to literature methods. $Cr(CO)_6$ (Strem), $Mo(CO)_6$ (Alfa), and $W(CO)_6$ (Strem) were used as received without further purification. Solution IR spectra were recorded in 0.1 mm path length CaF_2 cells on a Perkin-Elmer Model 1640 FTIR spectrophotometer. ^1H and ^{13}C were obtained on Bruker AF 300 and 250 spectrometers in THF-d_8. FAB mass spectral analyses were performed on a VG Analytical Autospec 3000 or Finnigan MAT 95 with 3-nitrobenzyl alcohol (*m*NBA) as a matrix. Elemental analyses were performed on a Carlo Erba Instruments NA 1500 Series 2 Analyzer.

Synthesis of $[PPN]_2[Cr_2(CO)_{10}]$. KC_8, 1.35 g (10 mmol), was suspended in 50 mL of THF. $Cr(CO)_6$, 2.2 g (10 mmol), was then added in one portion to the suspension. During the reaction, the flask was vented via an oil bubbler. Gas evolution ceased after approximately 2 h, and the mixture was filtered to remove the graphite. [PPN]Cl (6.5 g, 11 mmol) was added to precipitate the product, which was then isolated by filtration and dried under reduced pressure. Yield: 10.9 g (75% based on Cr). IR (cm^{-1}, MeCN): 1941 w sh, 1914 m, 1883 vs, 1790 m.

Synthesis of $[PPN]_2[Mo_2(CO)_{10}]$ and $[PPN]_2[W_2(CO)_{10}]$. The analogous dinuclear anions of the heavier group VI metals were synthesized a fashion similar to that described above for the chromium complex by substituting 2.64 g of $Mo(CO)_6$ or 3.52 g of $W(CO)_6$ for the $Cr(CO)_6$. The yields were 10.8 g (70%) and 11.2 g (65%), respectively. IR for $[PPN]_2[Mo_2(CO)_{10}]$ (cm^{-1}, MeCN): 1934 m, 1891 vs, 1792 m. IR for $[PPN]_2[W_2(CO)_{10}]$ (cm^{-1}, MeCN): 2041 w, 1937 s, 1884 vs, 1785 m.

Synthesis of $[PPN][Ph_2Bi\{Cr(CO)_5\}_2]$, ([PPN][1a]). $[PPN]_2[Cr_2(CO)_{10}]$, 1.46 g (1.0 mmol), was slurried in 50 mL of THF. Solid Ph_2BiCl, 0.40 g (1.0 mmol), was then added in one portion. The reaction proceeded rapidly with the color changing from orange-red to greenish yellow. As the reaction progressed, the yellow-orange transition metal salt dissolved and a fine gray precipitate formed. After being stirred for approximately 1 h to ensure complete reaction, the mixture was filtered through Celite to remove the precipitates and the solvent was concentrated *in vacuo* to approximately 10 mL. The product was then precipitated by the addition of a large volume of hexane (approximately 75 mL) to give a fine yellow powder, which was collected by filtration. Yield: 1.03 g (80% based on Bi). Crystals of suitable quality for X-ray diffraction studies were grown by dissolving the product in ether and then reducing the volume carefully until the first crystals began to form. Crystallization was then allowed to continue at −20 °C for several days. IR (THF, cm^{-1}): 2046 w, 2021 mw, 1929 vs, 1905 sh, 1890 m. ^1H NMR (THF-d_8, ppm): 7.48 m, 7.05 m. ^{13}C NMR (ppm): 227.0 (CO), 222.2 (CO), 139.0, 134.6, 131.7 d ($^1J_{P-C}$ = 208 Hz) 129.2, 128.9, 127.0, 126.14. MS (negative ion FAB , *m*NBA matrix): *m/z* 746.7 (M^-), 718.7, 690.7, 554.8. Anal. Calcd for $C_{58}H_{40}BiCr_2NO_{10}P_2$: C, 54.17; H, 3.14; N, 1.10. Found: C, 54.25; H, 3.23; N, 1.15.

Synthesis of $[PPN][Ph_2Bi\{Mo(CO)_5\}_2]$ ([PPN][1b]). The synthesis of [PPN][**1b**] was carried out in the same manner as described for [PPN]-[**1a**] using 1.55 g (1.0 mmol) of $[PPN]_2[Mo_2(CO)_{10}]$ and 0.40 g (1.0 mmol) of Ph_2BiCl. The yield was 0.96 g (70% based on Bi). IR (THF, cm^{-1}): 2057 w, 2041 mw, 1938 vs, 1917 mw, 1890 m. ^1H NMR (THF-d_8, ppm): 7.54 m, 7.06 m. ^{13}C NMR (ppm): 215.9 (CO), 211.0 (CO), 140.0, 134.6, 131.7 d ($^1J_{P-C}$ = 202 Hz) 129.2, 128.8, 127.5, 126.4. MS (negative ion FAB, *m*NBA): *m/z* 835 (M^-), 808, 780. Anal. Calcd for $C_{58}H_{40}BiMo_2NO_{10}P_2$: C, 50.70; H, 2.94; N, 1.02. Found: C, 49.61; H, 2.93; N, 1.35.

Synthesis of $[PPN][Ph_2Bi\{W(CO)_5\}_2]$ ([PPN][1c]). The preparation of [PPN][**1c**] was analogous to that of both [PPN][**1a**] and [PPN]-[**1b**] using 1.72 g (1.0 mmol) of $[PPN]_2[W_2(CO)_{10}]$ and 0.40 g (1.0 mmol) of Ph_2BiCl. The yield was 1.10 g (71% based on Bi). IR (THF, cm^{-1}): 2058 w, 2041 mw, 1931 vs, 1908 mw, 1888 m. ^1H NMR (THF-d_8, ppm): 7.50 m, 7.01 m. ^{13}C NMR (ppm): 203.9 (CO), 202.3 (CO), 139.2, 134.6, 131.8 d (J_{P-C} = 201 Hz) 129.0, 128.9, 127.6, 126.9. MS: (negative ion FAB, *m*NBA) 1011 (M-), 899, 878. Anal. Calcd for $C_{58}H_{40}BiNO_{10}P_2W_2$: C, 44.95; H, 2.60; N, 0.90. Found: C, 46.16; H, 2.85; N, 0.95.

Synthesis of $[Et_4N][Ph_2Bi\{Fe(CO)_4\}_2]$ ([Et$_4$N][2]). $[Et_4N]_2[Fe_2(CO)_8]$, 0.60 g (1.0 mmol), was suspended in 35−40 mL of THF, and 0.40 g (1.0 mmol) of Ph_2BiCl was dissolved in 25 mL of THF. The Ph_2BiCl solution was then added dropwise, over approximately 5 min, to the red suspension of the iron carbonylate with stirring. During the addition, the bright red solid $[Et_4N]_2[Fe_2(CO)_8]$ dissolved and a deep red solution was produced. The reaction was essentially complete at the end of the addition, but the reaction mixture was allowed to stir for an additional 1 h to ensure completion. After the solution was filtered through Celite to remove the organic salts produced, the solvent was removed *in vacuo* to yield a red oil. The product was isolated as deep red crystals by redissolving the oil in 10 mL of CH_2Cl_2 and layering the resultant solution with five volumes of ether. The crystals were collected by filtration to give 0.71 g (86% yield based on Bi). IR (cm^{-1}, THF): 2027 w, 2002 vs, 1980 vw, 1929 s, 1919 s. ^1H NMR (ppm, THF-d_8): 7.82 d (J = 6.5 Hz), 7.18 m, 3.21 q (J = 7.1 Hz), 1.24 t (J = 7.1 Hz). ^{13}C NMR (ppm, THF-d_8): 216.6 (CO), 137.6, 129.1 128.0, 52.9, 7.4. Anal. Calcd for $C_{28}H_{30}BiFe_2NO_8$: C, 40.6; H, 3.65; N, 1.69. Found: C, 41.2; H, 3.96; N, 1.96.

Synthesis of [PPN][2]. $[PPN][Ph_2BiFe(CO)_4]$, 100 mg (0.09 mmol), was dissolved in 30 mL of THF to produce a bright yellow solution. The addition of 50 mg (0.14 mmol) of solid $Fe_2(CO)_9$ caused the solution to change from yellow to red over approximately 90 min. After 2 h, the solution was filtered to remove the slight excess of $Fe_2(CO)_9$ remaining. The solvent, along with the volatile byproduct $Fe(CO)_5$, was removed under reduced pressure. The red solid residues extracted into 15 mL of ether were cooled to −20 °C. The resulting red needlelike crystals were isolated by filtration to yield 105 mg (94% based on Bi). IR (cm^{-1}, CH_2Cl_2): 2029 m, 2004 vs, 1982 w, 1923 vs.

Synthesis of $[PPN][Ph_2Bi\{Cr(CO)_5\}\{Fe(CO)_4\}]$ ([PPN][3]). A stock solution of $Cr(CO)_5THF$ was prepared by slurrying 0.75 g of hexacarbonylchromium in 50 mL of THF and irradiating with a 450-W medium-pressure mercury lamp for between 4 and 5 h. During irradiation, the solution changed from colorless to deep orange-red and all the solid dissolved. The final calculated concentration was 0.067 mol/L. $[PPN][Ph_2BiFe(CO)_4]$, 100 mg (0.09 mmol), was dissolved in 30 mL of THF to produce a bright yellow solution. Upon addition of 3 mL of the $Cr(CO)_5THF$ solution, the reaction mixture immediately changed from bright yellow to reddish-orange. The reaction mixture was allowed to stand for 30 min to ensure completion. Removal of the solvent under reduced pressure also removed volatile $Cr(CO)_6$, which was present as a minor impurity in the $Cr(CO)_5THF$ solution. The reddish-orange solid residues extracted into 15 mL of ether were cooled to −20 °C for several days. The resulting orange platelike crystals were isolated by filtration. Yield: 95 mg (84% based on Bi). IR (cm^{-1}, THF): 2045 mw, 2003 m, 1989 w, 1966 w, 1932 vs, 1922 sh, 1899 s, 1880 sh, 1869 sh. ^1H NMR (ppm, THF-d_8): 7.82 m, 7.61 m, 7.12 m, 3.39 q (J = 6.2 Hz), 1.12 t (J = 6.2 Hz). ^{13}C NMR (ppm, THF-d_8): 226.4 (CO), 221.0 (CO), 217.2 (CO), 139.0, 138.2, 134.5, 131.8, 129.0, 127.6, 127.5, 127.1.

Electrochemistry. The cyclic voltamograms for [PPN][**1**] were generated on a BAS 100 B/W electrochemical analyzer. The electrolyte solution used was 0.1 M tetra-*n*-butylammonium tetrafluoroborate in CH_2Cl_2 (dried over CaH_2 twice prior to use). All potentials were referenced to a Ag/AgCl electrode. For [PPN][**1a**], an irreversible oxidation process was observed at 0.95 V. This wave was partially obscured by another oxidation process at 1.0 V deriving from the cation.

(15) Shriver, D. F.; Drezdzon, M. A. *The Manipulation of Air Sensitive Compounds*; Wiley: New York, 1986.
(16) Ruff, J. K.; Sclientz, W. S. *Inorg. Synth.* **1975**, *15*, 84.
(17) Challenger, F.; Allpress, C. F. *J. Chem. Soc.* **1915**, *107*, 16.
(18) Sumner, C. E., Jr.; Collier, J. A.; Petit, R. *Organometallics* **1982**, *1*, 1350.
(19) Strong, H.; Krusic, P. J.; San Filippo, J., Jr. *Inorg. Synth.* **1990**, *28*, 203.
(20) Schwindt, M. A.; Lejon, T.; Hegedus, L. S. *Organometallics* **1990**, *9*, 2814.

The scans could only be run once without repolishing the electrode. It is believed that this problem is caused by the substrate being tested, or its oxidation products, coating the electrode surface during the oxidative wave. The complexes [PPN][**1b,c**] also show irreversible oxidation waves at 0.75 and 0.72 V, respectively.

Oxidation of [PPN][1] with Triflic Acid. A solution of triflic acid in acetonitrile was prepared by dissolving the acid in MeCN and diluting to a total volume of 55 mL to give a final concentration of 0.1 mmol/mL. [PPN][**1a**], 0.25 g (0.19 mmol), was then dissolved in 20 mL of CH_2Cl_2, and 1.9 mL of the prepared acid solution was added dropwise. The solution became momentarily red as the acid was added but returned to yellow a few minutes after the addition was complete. After 30 min of stirring, the solvent was removed *in vacuo*. The residues were extracted into ether to yield a pale yellow solution and a dark gray solid. The solution was filtered through a Celite pad to remove the fine solids. Removal of the ether *in vacuo* yielded a waxy yellow solid which was soluble in hexane. Cooling the hexane solution gave yellow crystals which were identified as $Cr(CO)_5(MeCN)$ (**4**) on the basis of their infrared spectrum. This assignment was confirmed by X-ray crystallography. A small number of colorless crystals were also collected and identified as Ph_3Bi by comparison of their ^1H NMR spectrum with an authentic sample. The reaction of [PPN][**1b**] and [PPN][**1c**] with triflic acid yielded $Mo(CO)_5(MeCN)$ and $W(CO)_5(MeCN)$, respectively, as the only carbonyl-containing products. These heavier analogs of **4** were identified by comparison of their infrared spectra with those of both **4** and authentic samples of the complexes prepared from $M(CO)_6$ (M = Cr, Mo, W) and Me_3NO.

Preparation of $M(CO)_5(MeCN)$ (M = Cr, Mo, W) with Me_3NO. The hexacarbonyl and 1 equiv of Me_3NO were weighed into the same flask. The combined solids were then dissolved in MeCN. The resulting solutions rapidly changed from colorless to bright yellow with accompanying evolution of gas. The IR spectra consist of two bands at 1950 and 1925 cm^{-1} consistent with a C_{4v} environment at the metal center. Removal of the solvent results in substantial decomposition to $M(CO)_6$ and metal. This decomposition is most severe for Mo, but even in this case, a small amount of the $M(CO)_5(MeCN)$ complex can be recovered upon extraction of the residues with hexane.

Oxidation of [PPN][1] with $Cu(MeCN)_4BF_4$. [PPN][**1a**], 0.25 g (0.19 mmol), and 0.062 g of $[Cu(MeCN)_4]BF_4$ (0.19 mmol) were placed in a flask. The flask was then charged with 30 mL of THF, and the mixture was allowed to stir overnight. The infrared spectrum of the solution indicated that the only carbonyl-containing material was **4**. The reactions with [PPN][**1b**] and [PPN][**1c**] gave analogous results producing $M(CO)_5(MeCN)$ (M = Mo and W, respectively).

X-ray Crystallography

General Considerations. All crystals were mounted with epoxy cement on the tip of a glass fiber. The data were collected using the TEXSAN Automatic Data Collection Series[21] on a Rigaku AFC5S diffractometer using Mo Kα radiation (λ = 0.710 69 Å). The crystallographic data collection and refinement parameters for each compound are summarized in Table 1. All data were collected at 223 K. The data were corrected for Lorentz and polarization effects, and for absorption using ψ-scans. Crystal and instrument stability were checked by measuring three standard reflections every 150 observations. The analytical form of the scattering factors for the appropriate neutral atoms were corrected for both the real ($\Delta f'$) and imaginary ($\Delta f''$) components of anomalous dispersion.[22] The residual R_1 calculated for refinements which were performed on F^2 is equal to the residual R calculated for refinements performed against F. This residual, R_1, is included to make comparisons between the two refinement methods more convenient. This scaling is necessary because, due to statistical factors, the residuals for refinement on F^2 are normally two to three times larger than those for the same refinement carried out on F.

Structure of [PPN][1a]. A small bright yellow rod of dimensions 0.2 × 0.2 × 0.4 mm^3 was chosen for data collection. The unit cell was determined from least-squares analysis of 25 reflections (6.50° ≤ 2θ ≤ 15.25°). The crystal system was determined to be triclinic, and the more common space group choice, $P\bar{1}$ (No. 2), was chosen on the basis of the intensity statistics. It was later shown to be correct by satisfactory refinement of the data. The locations of the heavy atoms were determined by direct methods with SHELXS-86.[23] The remaining atoms were located through successive least-squares refinements on F using the TEXSAN (5.0) structure solution package.[24] No decay correction was applied, as the standard reflections showed only random fluctuations. All of the non-hydrogen atoms were refined anisotropically, and the hydrogen atoms for both the cation and the anion were included in calculated positions. The final residuals of R = 0.0340 and wR = 0.0354 were based on 667 parameters and 5179 observed data ($I > 3\sigma(I)$). Selected positional and equivalent isotropic displacement parameters are included in Table 2, and selected interatomic bond distances and angles are given in Table 7.

Structure of [PPN][1b]. A yellow plate of dimensions 0.2 × 0.3 × 0.3 mm^3 was chosen for study. The unit cell was determined from 25 carefully centered reflections (4.75° ≤ 2θ ≤ 18.75°). The crystal system was determined to be triclinic, and the space group $P\bar{1}$ (No. 2) was selected on the basis of intensity statistics. Subsequent successful refinement showed the choice to be correct. The heavy atom positions were located by direct methods using SHELXS-86,[23] and the remaining atoms were located by successive least-squares refinements on F using the TEXSAN (5.0) structure solution package.[24] The non-hydrogen atoms were refined anisotropically and the hydrogen atoms on both the cation and the anion were included in calculated positions. The final residuals of R = 0.0556 and wR = 0.0607 were based on 667 parameters and 4871 observed data ($I > 3\sigma(I)$). Selected positional and equivalent isotropic displacement parameters are included in Table 3, and selected interatomic bond distances and angles are given in Table 7.

Structure of [PPN][1c]. A yellow block of dimensions 0.3 × 0.3 × 0.3 mm^3 was chosen for study. The unit cell was determined from least-squares analysis of 25 reflections (6.75° ≤ 2θ ≤ 17.25°). The crystal system was shown to be monoclinic, and the space group was chosen as $P2_1/n$ (No. 14) on the basis of systematic absences. The heavy atom positions were determined with SHELXS-86.[23] The remaining atoms were located by successive least-squares refinements on F using TEXSAN (5.0).[24] The bismuth, tungsten, phosphorus, oxygen, and nitrogen atoms were all refined anisotropically. The carbon atoms of the anion and the cation were refined isotropically while the lattice toluene was modeled as a rigid group. The hydrogen atoms associated with both the anion and the cation were included in calculated positions, but the contribution of the hydrogen atoms on the lattice solvent were ignored. Several residual electron density peaks persisted throughout the refinement. It appeared that these peaks were due to a significantly disordered molecule of ether at approximately half-occupancy in the lattice. It was possible to model the oxygen atom and the methylene carbon atoms satisfactorily; however, the disorder combined with the partial occupancy made it impossible to model the methyl carbons in a suitable manner. Therefore, the structural contribution of these two carbon atoms was also ignored. The final residuals of R = 0.068 and wR = 0.082 were based on 396 parameters and 3330 observed reflections ($I > 3\sigma(I)$). While the disorder problem did adversely affect the overall accuracy of the study, the errors associated with the geometry around the bismuth were comparable to those of the other structural studies reported here. Selected positional and equivalent isotropic displacement parameters are given in Table 4, and selected interatomic bond distances and angles are listed in Table 7.

Structure of [Et_4N][2]. A red cube 0.3 × 0.3 × 0.3 mm^3 in size was chosen for study. The unit cell was determined from 25 carefully centered reflections (6.75° ≤ 2θ ≤ 12.50°). The crystal system was determined to be monoclinic, and the space group $P2_1/n$ (No. 14) was selected on the basis of systematic absences. Subsequent successful refinement showed the choice to be correct. The heavy atom positions

(21) *Rigaku MSC Automatic Data Collection Control Software*, v 3.2.1; Molecular Structure Corp.: The Woodlands, TX, 1987.
(22) *International Tables for X-ray Crystallography*; Kynoch: Birmingham, England, 1974; Vol. 4, pp 99–101, 149–150.
(23) Sheldrick, G. M. In *Crystallographic Computing 3*; Sheldrick, G. M., Kruger, C., Goddard, R. Eds.; Oxford Press: Oxford, England, 1985; pp 175–189.
(24) TEXSAN: Single Crystal Structure Analysis Software, v. 5.0.
(25) *SHELXTL PC*, v 4.2; Siemens Crystallographic Research Systems: Madison, WI, 1990.

Table 1. Summary of Crystal Data for [PPN][**1a**−**c**], [Et_4N][**2**], [PPN][**3**], and **4**

	[PPN][**1a**]	[PPN][**1b**]	[PPN][**1c**]·C_7H_8·0.5$C_4H_{10}O$
empirical formula	$C_{58}H_{40}BiCr_2NO_{10}P_2$	$C_{58}H_{40}BiMo_2NO_{10}P_2$	$C_{64.6}H_{40}BiNO_{10.5}P_2W_2$
formula weight	1285.87	1373.76	1678.78
temp, K	223(2)	223(2)	223(2)
space group	$P\bar{1}$ (No. 2)	$P\bar{1}$ (No.2)	$P2_1/n$ (No. 14)
a, Å	12.622(6)	12.738(4)	9.833(5)
b, Å	12.800(6)	12.967(3)	28.166(10)
c, Å	16.798(6)	16.817(7)	24.037(14)
α, deg	84.05(3)	84.60(3)	
β, deg	87.89(3)	87.95(3)	94.79(5)
γ, deg	88.86(3)	88.38(3)	
V, Å^3	2697.3(3.7)	2762.9(3.0)	6634.3(5.7)
Z	2	2	4
ϱ_{calc} g/cm^3	1.58	1.65	1.67
μ, mm^{-1}	3.74	3.72	6.27
F(000)	1272	1344	3228
T_{max}/T_{min}	1.000/0.677	1.000/0.837	1.000/0.824
crystal size, mm^3	0.2 × 0.2 × 0.4	0.2 × 0.2 × 0.3	0.3 × 0.3 × 0.3
crystal color/shape	yellow rod	yellow plate	yellow block
refinement method	*F*	*F*	*F*
goodness-of-fit	1.066	1.808	1.707
residuals[a]	R = 0.0340	R = 0.0556	R = 0.0683
	wR = 0.0354	wR = 0.0607	wR = 0.0816

	[Et_4N][**2**]	[PPN][**3**]·0.48$C_4H_{10}O$	**4**
empirical formula	$C_{28}H_{30}BiFe_2NO_8$	$C_{58.92}H_{44.8}BiCrFeNO_{9.48}P_2$	$C_7H_3CrNO_5$
formula weight	829.21	1297.3	233.10
temp, K	223(2)	223(2) K	223(2) K
space group	$P2_1/n$ (No. 14)	$P\bar{1}$ (No.2)	$P\bar{1}$ (No. 2)
a, Å	13.064(3)	10.998(2)	6.2140(10)
b, Å	14.309(3)	16.244(3)	12.167(2)
c, Å	16.951(3)	17.203(3)	13.402(3)
α, deg		85.60(3)	85.38(3)
β, deg	100.21(3)	76.42(3)	86.84(3)
γ, deg		80.13(3)	86.30(3)
V, Å^3	3118.5(1.1)	2941.1(9)	1006.6(3)
Z	4	2	4
ϱ_{calc}, g/cm^3	1.77	1.46	1.54
μ, mm^{-1}	6.59	3.51	1.13
F(000)	1616	1288.32	464
T_{max}/T_{min}	1.000/0.654	1.000/0.806	
crystal size, mm^3	0.3 × 0.3 × 0.3	0.3 × 0.1 × 0.3	0.1 × 0.1 × 0.4
crystal color/shape	red cube	orange plate	pale yellow needle
refinement method	F^2	F^2	F^2
Goodness-of-fit	1.031	0.946	1.059
residuals[a]	R_1 = 0.0310	R_2 = 0.0424	R_1 = 0.0460
	wR_2 = 0.0679	wR_2 = 0.1259	wR_2 = 0.0905

[a] The residuals are defined as follows: $wR_2 = [\Sigma\{w(F_o^2 - F_c^2)^2\}/\Sigma\{wF_o^2)^2\}]^{0.5}$, with $w = [\Sigma^2F_o^2 + (aP)^2 + bP]^{-1}$ and $P = 0.33F_o^2 + 0.67F_c^2$; $R_1 = R = \Sigma||F_o| - |F_c||/\Sigma|F_o|$; $wR = [\Sigma w||F_o| - |F_c||^2/\Sigma|F_o|^2]^{0.5}$, with $w = [\sigma^2(F_o)]^{-1}$.

were located by direct methods using the SHELXTL-PC software package,[25] and the remaining atoms were located by successive least-squares refinements on F^2 using SHELXL-93.[26] The non-hydrogen atoms were refined anisotropically, and the hydrogen atoms were included in calculated positions using a riding model. During the final stages of refinement, the combination of large displacement ellipsoids for the methylene carbons of the cation and persistent residual peaks in the difference map suggested that the cation was not fully ordered. A second set of methylene positions was added to the model and the sum of the populations for each pair of positions constrained to unity. The relative population of the two positions was found to be 0.62:0.38. The final residuals of $R_1(F) = 0.0310$ and $wR_2(F^2) = 0.0744$ were based on 397 parameters and 5521 observed data ($I > 2\sigma(I)$). Selected positional and equivalent isotropic displacement parameters are given in Table 5, while selected interatomic bond distances and angles for the anion may be found in Table 7.

Structure of [PPN][3]·0.48Et_2O. An orange plate 0.3 × 0.1 × 0.3 mm^3 in size was chosen for study. The unit cell was determined from 25 carefully centered reflections (7.25° ≤ 2*θ* ≤ 12.25°). The crystal system was determined to be triclinic, and the space group $P\bar{1}$ (No. 2) was selected on the basis of intensity statistics. Subsequent successful refinement showed the space group choice to be correct. The heavy atom positions were located by direct methods using the SHELXTL-PC software package,[25] and the remaining atoms were located by successive least-squares refinements on F^2 using SHELXL-93.[26] A molecule of lattice ether was also found during the later stages of refinement. The lattice solvent positions were found to be ordered, but the occupancy was found to be less than 1. Refinement of the occupancy led to convergence at a value of 0.485. The lattice solvent was refined isotropically, and the contribution of the hydrogen atoms associated with it was ignored. The remaining non-hydrogen atoms were refined anisotropically, and the hydrogen atoms associated with both the cation and the anion were included in calculated positions using a riding model with a fixed displacement parameter. The final residuals of $R_1(F) = 0.0424$ and $wR_2(F^2) = 0.1426$ were based on 669 parameters and 7265 observed data ($I > 2\sigma(I)$). Selected positional and equivalent isotropic displacement parameters are included in Table 6, and selected interatomic bond distances and angles are given in Table 7.

Structure of 4. A pale yellow needle 0.1 × 0.1 × 0.4 mm^3 in size was chosen for data collection. The cell constants were determined by a least-squares refinement of 18 carefully centered reflections (6.50° ≤ 2*θ* ≤ 22.25°). The crystal system was determined to be triclinic,

(26) Sheldrick, G. M. SHELXL-93. University of Göttingen, Germany, 1993.

Table 2. Selected Positional and Displacement Parameters for [PPN][**1a**]

atom	*x*	*y*	*z*	*B*(eq), Å^2
Bi(1)	−0.42697(2)	0.61329(2)	0.72960(2)	2.72(1)
Cr(1)	−0.2265(1)	0.6691(1)	0.67333(7)	3.18(7)
Cr(2)	−0.4873(1)	0.4144(1)	0.78949(7)	3.17(7)
O(11)	−0.2398(5)	0.5255(5)	0.5419(4)	6.1(4)
O(12)	−0.3183(6)	0.8512(5)	0.5668(4)	6.9(5)
O(13)	−0.2094(5)	0.8173(5)	0.8014(4)	6.0(4)
O(14)	−0.1429(5)	0.4957(5)	0.7938(3)	5.3(4)
O(15)	−0.0084(5)	0.7156(5)	0.6075(4)	5.8(4)
O(21)	−0.6175(5)	0.4047(5)	0.6420(4)	5.5(4)
O(22)	−0.2988(5)	0.3317(5)	0.6972(3)	5.2(4)
O(23)	−0.3561(6)	0.4332(5)	0.9341(4)	6.8(4)
O(24)	−0.6833(5)	0.5045(5)	0.8684(4)	6.7(4)
O(25)	−0.5412(4)	0.1943(4)	0.8533(4)	4.7(3)
C(11)	−0.2369(6)	0.5782(7)	0.5930(5)	4.0(5)
C(12)	−0.2859(7)	0.7812(7)	0.6060(5)	4.6(5)
C(13)	−0.2171(7)	0.7603(7)	0.7533(5)	4.0(5)
C(14)	−0.1745(7)	0.5600(7)	0.7472(5)	3.7(5)
C(15)	−0.0939(7)	0.6994(6)	0.6336(5)	3.8(5)
C(21)	−0.5684(7)	0.4098(6)	0.6969(5)	3.9(5)
C(22)	−0.3689(7)	0.3650(6)	0.7328(5)	3.5(5)
C(23)	−0.4056(7)	0.4284(6)	0.8793(5)	4.0(5)
C(24)	−0.6084(7)	0.4715(6)	0.8395(5)	4.3(5)
C(25)	−0.5215(6)	0.2789(7)	0.8280(5)	3.6(5)
C(101)	−0.5448(6)	0.6604(6)	0.6342(4)	2.9(4)
C(102)	−0.6489(6)	0.6816(6)	0.6556(4)	3.5(4)
C(103)	−0.7242(6)	0.7000(6)	0.5976(6)	4.1(5)
C(104)	−0.6961(7)	0.6962(6)	0.5190(5)	4.2(5)
C(105)	−0.5940(7)	0.6739(8)	0.4979(5)	5.0(6)
C(106)	−0.5181(6)	0.6571(7)	0.5548(5)	4.2(5)
C(201)	−0.4828(6)	0.7351(6)	0.8109(4)	3.2(4)
C(202)	−0.4830(7)	0.8384(7)	0.7793(5)	4.3(5)
C(203)	−0.5079(8)	0.9186(7)	0.8257(6)	5.3(6)
C(204)	−0.5353(7)	0.8948(8)	0.9054(6)	5.1(6)
C(205)	−0.5367(7)	0.7919(8)	0.9361(5)	4.8(6)
C(206)	−0.5106(6)	0.7124(7)	0.8903(5)	4.0(5)

Table 3. Selected Positional and Displacement Parameters for [PPN][**1b**]

atom	*x*	*y*	*z*	*B*(eq), Å^2
Bi(1)	−0.42455(5)	0.61373(4)	0.72991(4)	2.66(3)
Mo(1)	−0.2172(1)	0.6693(1)	0.66965(8)	2.90(7)
Mo(2)	−0.4869(1)	0.4088(1)	0.79232(8)	3.04(7)
O(11)	−0.234(1)	0.516(1)	0.5329(8)	6.5(9)
O(12)	−0.312(1)	0.858(1)	0.5559(8)	7(1)
O(13)	−0.198(1)	0.827(1)	0.8021(8)	6.2(9)
O(14)	−0.135(1)	0.491(1)	0.7966(8)	5.8(8)
O(15)	0.008(1)	0.708(1)	0.6018(8)	5.5(8)
O(21)	−0.621(1)	0.402(1)	0.6370(8)	5.5(8)
O(22)	−0.291(1)	0.326(1)	0.6944(7)	5.5(8)
O(23)	−0.346(1)	0.429(1)	0.9415(9)	8(1)
O(24)	−0.692(1)	0.4994(9)	0.8750(8)	6.0(8)
O(25)	−0.539(1)	0.1820(9)	0.8586(8)	5.3(7)
C(11)	−0.230(1)	0.571(1)	0.583(1)	4(1)
C(12)	−0.280(1)	0.789(1)	0.597(1)	4(1)
C(13)	−0.205(1)	0.770(1)	0.755(1)	4(1)
C(14)	−0.162(1)	0.553(1)	0.751(1)	3.3(9)
C(15)	−0.075(1)	0.695(1)	0.626(1)	4(1)
C(21)	−0.574(1)	0.404(1)	0.692(1)	4(1)
C(22)	−0.362(1)	0.355(1)	0.732(1)	4(1)
C(23)	−0.398(2)	0.423(1)	0.887(1)	5(1)
C(24)	−0.618(1)	0.467(1)	0.845(1)	5(1)
C(25)	−0.521(1)	0.268(1)	0.833(1)	4(1)
C(101)	−0.541(1)	0.661(1)	0.634(1)	3.0(8)
C(102)	−0.646(1)	0.680(1)	0.657(1)	4(1)
C(103)	−0.721(1)	0.699(1)	0.599(1)	5(1)
C(104)	−0.691(1)	0.698(1)	0.519(1)	4(1)
C(105)	−0.588(1)	0.681(1)	0.497(1)	5(1)
C(106)	−0.514(1)	0.663(1)	0.556(1)	4(1)
C(201)	−0.482(1)	0.738(1)	0.811(1)	3.0(9)
C(202)	−0.474(1)	0.840(1)	0.779(1)	5(1)
C(203)	−0.501(1)	0.916(1)	0.831(1)	6(1)
C(204)	−0.535(1)	0.893(2)	0.909(1)	6(1)
C(205)	−0.539(1)	0.792(2)	0.938(1)	6(1)
C(206)	−0.512(1)	0.714(1)	0.887(1)	4(1)

and the more common space group, $P\bar{1}$ (No. 2), was selected on the basis of intensity statistics. This choice was shown to be correct by subsequent successful refinement. All the atoms were located during the initial structure solution by direct methods using the SHELXTL-PC software package.[25] Least-squares refinement of the structure was carried out on F^2 using SHELXL-93.[26] The final residuals were $R_1(F) = 0.046$ and $wR_2(F^2) = 0.090$ for 253 parameters and 1710 observed data ($I > 2\sigma(I)$). The positional and displacement parameters along with the complete interatomic bond distances and angles are included in the supplementary material.

Results

Syntheses. The dinuclear group 4 anions used as starting materials in this work are conveniently synthesized by a modification of the procedure reported by Hegedus and coworkers[20] for the synthesis of $[Cr(CO)_5]^{2-}$. This simple method of preparation allows these anions to be easily isolated from solution by precipitation with [PPN]Cl in isolated yields ranging from 65% to 75%.

When Ph_2BiCl, either as a solid or in THF solution, is added to a slurry of any of the group VI metal carbonylates in THF, the solution rapidly changes from red-orange to bright yellow. If the Ph_2BiCl is added to a slurry of the $[Et_4N]_2[Fe_2(CO)_8]$, the resultant solution is deep red. In all cases, the starting transition metal salt completely dissolves while a fine gray precipitate, presumably [PPN]Cl or $[Et_4N]Cl$, forms as the reaction progresses. [PPN][**1a**−**c**] can be precipitated as bright yellow powders from concentrated THF solutions by adding excess hexane in 80%, 70%, and 71% yields, respectively. $[Et_4N]$[**2**] is most conveniently isolated by precipitating it from dichloromethane solution with excess ether to give a dark red powder in 86% yield. [PPN][**2**] can be purified easily by dissolving it in ether and allowing the solution to stand at −20 °C for several days to produce red needlelike crystals.

As expected the $[PPN]^+$ salts of all the clusters show similar physical properties. They are insoluble in hydrocarbons, sparingly soluble in weakly polar solvents such as toluene and ether, and completely soluble in polar solvents such as THF, CH_2Cl_2, or CH_3CN. The $[Et_4N]^+$ salt of $[\mathbf{2}]^-$ is insoluble in ether and toluene but is soluble in CH_2Cl_2 and most other polar organic solvents. Except in the case of $[Et_4N]$[**2**], crystals suitable for X-ray diffraction studies were obtained from ethereal solutions held at −20 °C for several days. Crystals of $[Et_4N]$[**2**] were grown by layering a concentrated dichloromethane solution with four to five volumes of ether.

The ^1H NMR spectra of all five organobismuth clusters are essentially identical and therefore of little diagnostic value. They consist of two complex multiplets in the aromatic region centered at 7.5 and 7.0 ppm. The lower field signal is primarily due to the presence of the $[PPN]^+$ cation while the higher field signal is a result of the phenyl rings on the bismuth center. The ^{13}C spectra of all five clusters are also very similar to each other in the phenyl region but show distinct differences in the carbonyl region (Table 8). The carbonyl region of the ^{13}C spectrum of $[\mathbf{3}]^-$ looks like a superposition of that of $[\mathbf{1a}]^-$ and $[\mathbf{2}]^-$. Negative ion FAB mass spectra of [PPN][**1**] clearly show parent ions with the correct isotopic distribution patterns for compounds containing two metals. The IR spectra of the group VI clusters, $[\mathbf{1}]^-$, all show a pattern indicative of the presence of a $M(CO)_5$ fragment. The spectrum of $[\mathbf{2}]^-$ is identical in pattern to that seen for $[Ph_2BiFe(CO)_4]^-$ [8] with a shift of energy of approximately 20 cm^{-1} higher due to delocalization of the cluster charge over more atoms. As expected, the IR spectrum of the

Table 4. Selected Positional and Displacement Parameters for [PPN][1c]·C_7H_8·0.5$C_4H_{10}O$

atom	x	y	z	B(eq), Å²
Bi(1)	−0.0767(2)	0.25077(6)	0.07073(6)	3.24(7)
W(1)	0.0880(2)	0.16625(6)	0.06404(7)	3.35(8)
W(2)	−0.3311(2)	0.27026(6)	0.00591(7)	3.31(8)
O(11)	−0.183(3)	0.116(1)	0.016(1)	8(2)
O(12)	0.020(3)	0.139(1)	0.184(1)	7(2)
O(13)	0.343(3)	0.222(1)	0.120(1)	7(2)
O(14)	0.156(3)	0.193(1)	−0.058(1)	9(2)
O(15)	0.249(3)	0.0705(9)	0.058(1)	5(2)
O(21)	−0.460(3)	0.174(1)	0.042(1)	8(2)
O(22)	−0.189(4)	0.215(1)	−0.090(1)	10(2)
O(23)	−0.226(4)	0.370(1)	−0.032(1)	10(2)
O(24)	−0.442(3)	0.323(1)	0.107(1)	8(2)
O(25)	−0.593(3)	0.285(1)	−0.074(1)	11(3)
C(11)	−0.086(4)	0.135(1)	0.035(2)	4(1)
C(12)	0.044(5)	0.152(2)	0.140(2)	5(1)
C(13)	0.249(4)	0.201(1)	0.100(2)	4(1)
C(14)	0.132(4)	0.180(2)	−0.014(2)	6(1)
C(15)	0.185(5)	0.108(2)	0.061(2)	6(1)
C(21)	−0.405(4)	0.211(2)	0.030(2)	5(1)
C(22)	−0.248(4)	0.235(2)	−0.055(2)	6(1)
C(23)	−0.260(4)	0.334(2)	−0.020(2)	4.0(9)
C(24)	−0.395(5)	0.300(2)	0.071(2)	6(1)
C(25)	−0.503(4)	0.279(1)	−0.044(2)	5(1)
C(101)	−0.101(3)	0.258(1)	0.160(1)	3.3(8)
C(102)	−0.225(3)	0.247(1)	0.184(1)	3.3(8)
C(103)	−0.239(4)	0.246(1)	0.241(2)	5(1)
C(104)	−0.125(5)	0.256(2)	0.277(2)	6(1)
C(105)	−0.005(3)	0.266(1)	0.255(1)	3.3(8)
C(106)	0.006(3)	0.266(1)	0.200(1)	3.3(8)
C(201)	0.045(4)	0.317(1)	0.066(2)	4.3(9)
C(202)	0.008(3)	0.360(1)	0.084(1)	3.1(8)
C(203)	0.076(4)	0.403(1)	0.079(2)	5(1)
C(204)	0.204(4)	0.398(1)	0.054(1)	3.4(8)
C(205)	0.249(4)	0.358(2)	0.035(2)	5(1)
C(206)	0.178(4)	0.316(1)	0.040(2)	4(1)

mixed-metal cluster, $[3]^-$, looks essentially like a superposition of those associated with the homometallic clusters.

Structures of [PPN][1a−c], [Et₄N][2], and [PPN][3]. The data collection and refinement parameters for all five structures are summarized in Table 1, while the positional and displacement parameters for the anion of each salt are listed in Tables 2−6. Figures 1−3 show the molecular geometries of $[\mathbf{1a}]^-$, $[\mathbf{2}]^-$, and $[\mathbf{3}]^-$, respectively. Diagrams of $[\mathbf{1b}]^-$ and $[\mathbf{1c}]^-$ are included with the supplementary material since they are isostructural with $[\mathbf{1a}]^-$. As can be seen from the diagrams, all of the anions contain a bismuth atom which is surrounded by two phenyl rings and two metal−carbonyl fragments in a distorted tetrahedral geometry. The angles are distorted from ideal tetrahedral values by an expansion of the M−Bi−M angles to approximately 125° and a corresponding contraction of the C−Bi−C angles to 94.5° (Table 7). The C−Bi−M angles, however, remain clustered around the ideal tetrahedral angle, ranging from 103 to 112°. The Bi−M and Bi−C distances are also tabulated in Table 7.

Electrochemistry and Oxidation of [PPN][1]. In dichloromethane, the [PPN][1] complexes all display an irreversible oxidation wave between 0.70 and 0.90 V relative to Ag/AgCl. Quantitative measurement of the potentials is complicated by the presence of an oxidation wave due to the cation at roughly the same potential. Because of this electrochemical behavior, it was of interest to examine the products of chemical oxidation of [PPN][1]. Two different approaches were examined: reactions with $Cu(MeCN)_4BF_4$ and triflic acid as the oxidants. With either method, complete degradation of the cluster occurs in all three cases to yield $M(CO)_5(MeCN)$ as the only carbonyl-containing product. For chromium this result was confirmed by crystallographic analysis. The molybendum and tungsten

Table 5. Atomic coordinates (×10⁴) and Equivalent Isotropic Displacement Parameters (Å² × 10³) for [Et₄N][2]

atom	x	y	z	U(eq)[a]
Bi(1)	1303(1)	7440(1)	8572(1)	24(1)
Fe(1)	2191(1)	5863(1)	9105(1)	32(1)
Fe(2)	548(1)	7691(1)	7043(1)	29(1)
O(11)	248(5)	4826(4)	8582(4)	97(2)
O(12)	2532(4)	6571(4)	10753(3)	65(2)
O(13)	3694(4)	6146(4)	8029(4)	74(2)
O(14)	3302(5)	4165(4)	9664(3)	82(2)
O(21)	−674(5)	5984(4)	7066(3)	79(2)
O(22)	2717(4)	7753(4)	6818(3)	61(1)
O(23)	−413(5)	9466(4)	7371(3)	72(2)
O(24)	−141(4)	7838(4)	5317(3)	74(2)
C(11)	992(6)	5263(5)	8770(5)	55(2)
C(12)	2384(5)	6320(5)	10098(4)	45(2)
C(13)	3099(5)	6064(4)	8445(4)	42(2)
C(14)	2861(6)	4838(5)	9440(4)	50(2)
C(21)	−192(5)	6649(5)	7074(4)	44(2)
C(22)	1870(5)	7719(4)	6917(3)	39(2)
C(23)	−27(5)	8765(5)	7258(4)	42(2)
C(24)	110(5)	7796(5)	5995(4)	47(2)
C(101)	127(4)	7808(4)	9346(3)	26(1)
C(102)	−233(5)	8707(4)	9374(4)	36(1)
C(103)	−952(5)	8941(5)	9853(4)	43(2)
C(104)	−1313(5)	8257(5)	10309(4)	46(2)
C(105)	−954(5)	7357(4)	10296(4)	42(2)
C(106)	−236(4)	7123(4)	9821(3)	33(1)
C(201)	2329(4)	8691(4)	8956(3)	26(1)
C(202)	2443(5)	9373(4)	8411(4)	36(1)
C(203)	3089(5)	10139(4)	8648(4)	46(2)
C(204)	3598(5)	10213(4)	9415(4)	45(2)
C(205)	3476(5)	9533(5)	9967(4)	48(2)
C(206)	2847(5)	8767(4)	9741(4)	40(2)

[a] U(eq) is defined as one-third of the trace of the orthogonalized U_{ij} tensor.

analogs were identified by comparison of their infrared spectra with that of the chromium compound, as well as with those of authentic samples generated from $M(CO)_6$ and Me_3NO in acetonitrile. Additionally the reaction of $[\mathbf{1}]^-$ with either oxidant produces a fine gray metallic precipitate along with small amounts of triphenylbismuth and a small amount of benzene. The triphenylbismuth and benzene were identified by their ^1H NMR spectra. When the protonations were carried out at −78 °C and followed by ^1H NMR, no signals consistent with the presence of a metal hydride were detected.

Structure of 4. **4** crystallizes in the space group $P\bar{1}$ with $Z = 4$. There are no significant intermolecular contacts between the two independent molecules in the asymmetric unit. The chromium atom displays the expected pseudo-octahedral geometry. The average M−C bond distances, 1.842(7) Å (*trans* to MeCN), 1.903(8) Å (*cis* to MeCN), and M−N bond distances, 2.065(1) Å (average), all fall within the expected ranges.

Discussion

The reaction of Ph_2BiCl with the mononuclear transition metal anions $[Mn(CO)_5]^-$ and $[Fe(CO)_4]^{2-}$ has been shown to yield $Ph_2BiMn(CO)_5$ and $[Ph_2BiFe(CO)_4]^-$ via halide substitution reactions.[8] In both of these cases, the bismuth atom is three-coordinate and retains a lone pair. The early reactivity studies performed on these species suggested that the lone pair is neither nucleophilic nor basic. In contrast, when dinuclear anions such as $[M_2(CO)_{10}]^{2-}$ (M = Cr, Mo, W) or $[Fe_2(CO)_8]^{2-}$ are used instead of mononuclear anions the bismuth binds a second metal fragment with this "inert" lone pair.

The clusters $[\mathbf{1}]^-$ are all isoelectronic and isostructural, consisting of a bismuth atom surrounded by two phenyl rings and two $M(CO)_5$ fragments in a distorted tetrahedral geometry. The $M(CO)_5$ fragments possess the expected pseudo-octahedral

Table 6. Atomic Coordinates (x10^4) and Equivalent Isotropic Displacement Parameters (Å^2 × 10^3) for [PPN][**3**]·0.48Et_2O

atom	*x*	*y*	*z*	*U*(eq)[a]
Bi(1)	3253(1)	7582(1)	3842(1)	38(1)
Fe(1)	2833(1)	8225(1)	2461(1)	50(1)
Cr(1)	1991(1)	6374(1)	4678(1)	42(1)
O(11)	3953(10)	6605(6)	1770(6)	103(3)
O(12)	4366(12)	9486(7)	2557(8)	131(4)
O(13)	123(9)	8407(6)	3254(6)	87(3)
O(14)	2366(12)	9009(6)	962(5)	114(4)
O(21)	4170(9)	4964(6)	4110(6)	91(3)
O(22)	1112(7)	6117(5)	3180(5)	75(2)
O(23)	−240(8)	7747(6)	5213(5)	82(2)
O(24)	3144(7)	6578(5)	6073(4)	71(2)
O(25)	473(8)	5178(6)	5709(5)	86(3)
C(11)	3522(12)	7244(8)	2052(7)	71(3)
C(12)	3804(13)	8991(8)	2547(8)	78(4)
C(13)	1193(13)	8344(7)	2948(7)	64(3)
C(14)	2532(13)	8711(7)	1547(7)	73(3)
C(21)	3344(11)	5508(7)	4319(7)	61(3)
C(22)	1425(10)	6218(7)	3759(7)	55(3)
C(23)	582(10)	7239(7)	5008(6)	53(3)
C(24)	2690(9)	6530(6)	5549(6)	48(2)
C(25)	1031(10)	5624(7)	5299(7)	59(3)
C(101)	2986(9)	8717(6)	4583(5)	44(2)
C(102)	3822(10)	8819(7)	5032(6)	57(3)
C(103)	3657(12)	9531(8)	5462(6)	69(3)
C(104)	2632(13)	10137(8)	5460(6)	69(3)
C(105)	1782(11)	10040(7)	5030(6)	65(3)
C(106)	1929(10)	9339(6)	4580(6)	53(3)
C(201)	5358(8)	7277(6)	3752(5)	43(2)
C(202)	5794(9)	6693(7)	4260(6)	55(3)
C(203)	7095(10)	6513(8)	4284(7)	71(3)
C(204)	7942(11)	6929(9)	3773(8)	75(4)
C(205)	7502(11)	7513(8)	3258(9)	86(4)
C(206)	6228(11)	7683(8)	3229(8)	75(4)

[a] *U*(eq) is defined as one- third of the trace of the orthogonalized U_{ij} tensor.

C_{4v} symmetry. The nature and degree of the tetrahedral distortion at bismuth are similar for all three group VI complexes with the M−Bi−M angle expanding to an average of 125.7-(4)° while the C−Bi−C angle contracts to an average of 94.5-(6)°. The M−Bi−C angles are normal for tetrahedral coordination, ranging from 103.8(2) to 112.3(4)°.

The diiron cluster [**2**]$^-$ and the heterometallic cluster [**3**]$^-$ both show a similar distortion in the tetrahedral coordination at the bismuth center. However, the slightly smaller steric bulk of the $Fe(CO)_4$ fragment appears to allow for a smaller M−Bi−M angle in these clusters. The Cr−Bi−Fe angle in [**3**]$^-$ is 122.35(5)° and the Fe−Bi−Fe angle in [**2**]$^-$ is only 121.46-(3)°. Even though the M−Bi−M angle is not as large, the C−Bi−C angle remains the same as that seen for the series of group VI clusters (94.5°) and the C−Bi−M angles still range from 103.3(2) to 112.3(2)°.

A similar contraction of the C−Bi−C bond angles has been noted for other metalated organobismuth complexes as well as for trimethyl- and triphenylbismuth (Table 9). In earlier studies on organobismuth compounds,[27] it has been suggested that the observed geometry was due to the lone pair of electrons residing in an orbital of primarily s character in keeping with the "inert pair" idea for heavier main-group metals. Correspondingly, it was thought that the bonds to the carbon atoms were made by orbitals of primarily p character, thereby resulting in the observed bond angles which are close to 90°. In the case of the four-coordinate $Ph_3BiCr(CO)_5$, it was postulated that the bismuth−chromium donor bond is made with an orbital on bismuth which has primarily s character.[5] The presence of four

(27) (a) Hawley, D. M.; Ferguson, G. *J. Chem. Soc.* **1968**, 2059. (b) Beagley, B.; McAloon, K. T. *J. Mol. Struct.* **1973**, *17*, 429.

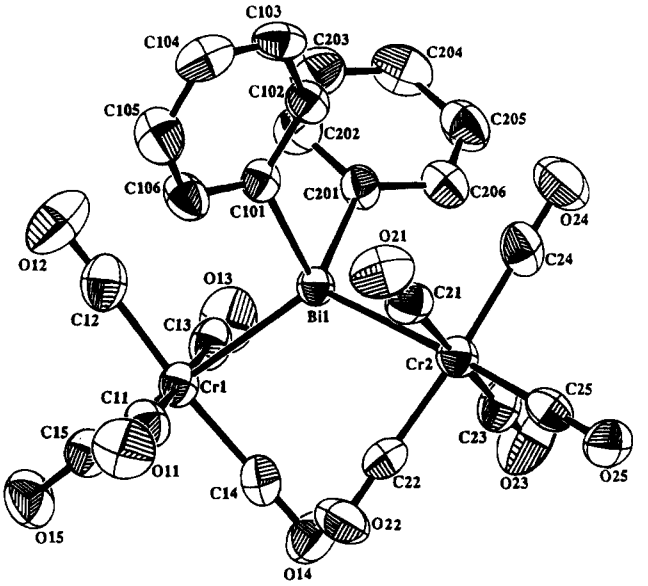

Figure 1. Diagram of the anion of [PPN][**1a**] showing the displacement ellipsoids (50% probability level) and the atomic labeling scheme.

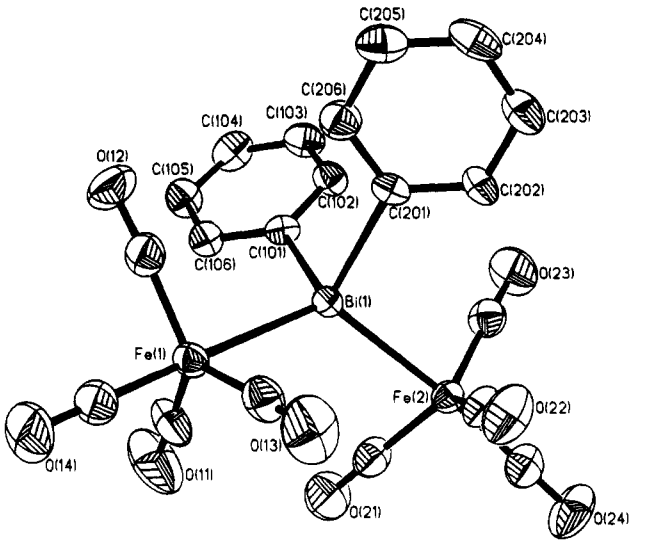

Figure 2. Diagram of the anion of [Et_4N][**2**] showing the displacement ellipsoids (50% probability level) and the atomic labeling scheme.

bonds to bismuth in [**1**]$^-$, [**2**]$^-$, and [**3**]$^-$ requires bismuth to use the s as well as p orbitals, although the orbitals created are not best described as ideal sp^3 hybrids, given the distortion of the bond angles away from ideal tetrahedral values. The distortion may be induced by steric factors although electronic considerations may also be important as will be discussed shortly. The steric argument is consistent with the smaller contraction of the M−Bi−M bond which is observed with the substitution of a less bulky $Fe(CO)_4$ fragment for a $M(CO)_5$ fragment. It is also interesting to note that the M−C−M bond angle remains essentially constant for the series [**1a−c**]$^-$ which implies, if size is the dominant feature, that the greater steric demand caused by the lengthening of the $M-C_{CO}$ bonds, as the size of M increases, is almost completely offset by the increase in the Bi−M bond length.

Comparison of the Bi−Cr bond distances in [**1a**]$^-$ with those of the only other structurally characterized organobismuth−chromium complex, $Ph_3BiCr(CO)_5$, further supports the view that the bismuth atom in [**1a**]$^-$ is sp^3 hybridized. A mostly covalent bond such as that found in [**1a**]$^-$ would be expected to be shorter than a dative bond such as that seen in $Ph_3BiCr(CO)_5$. Comparison of the two values—2.750(2) Å for [**1a**]$^-$

Table 7. Selected Bond Metricals for [**1a−c**]$^-$, [**2**]$^-$, and [**3**]$^-$

	Distances (Å)			
complex	Bi−M	Bi−C	av M−C	av C−O
[**1a**]$^-$	2.750(2)	2.254(7)	1.87(3)	1.146(9)
	2.750(2)	2.263(7)		
[**1b**]$^-$	2.882(2)	2.25(1)	2.02(4)	1.14(2)
	2.885(2)	2.30(1)		
[**1c**]$^-$	2.891(2)	2.20(3)	1.98(5)	1.17(4)
	2.997(3)	2.23(4)		
[**2**]$^-$	2.6237(9)	2.251(5)	1.778(12)	1.147(6)
	2.6294(10)	2.262(5)		
[**3**]$^-$ (Fe)	2.630(2)	2.254(9)	1.785(17)	1.14(2)
(Cr)	2.722(2)	2.260(9)	1.88(2)	

	Angles (deg)			
complex	M−Bi−M	C−Bi−C	M−Bi−C	av M−C−O
[**1a**]$^-$	125.48(5)	95.2(3)	109.6(2), 106.7(2), 103.8(2), 111.8(2)	177.8(6)
[**1b**]$^-$	125.59(5)	94.2(5)	108.8(4), 107.1(4), 104.2(3), 112.3(4)	178(1)
[**1c**]$^-$	126.21(7)	94(1)	103.9(9), 112(1), 110.5(9), 105.0(9)	176(2)
[**2**]$^-$	121.46(3)	94.5(2)	107.84(14), 112.25(14), 111.53(14), 105.97(14)	177.3(1.3)
[**3**]$^-$	122.35(5)	94.5(3)	109.3(2), 103.3(2), 112.3(2), 111.1(2)	177.6(1.4)

Table 8. Selected ^{13}C NMR Signals (ppm) for the Carbonyl Ligands in [**1a−c**]$^-$, [**2**]$^-$, and [**3**]$^-$

complex	carbonyl carbons
$[Ph_2Bi\{Cr(CO)_5\}_2]^-$	227.0, 222.2
$[Ph_2Bi\{Mo(CO)_5\}_2]^-$	215.9, 211.0
$[Ph_2Bi\{W(CO)_5\}_2]^-$	203.9, 202.3
$[Ph_2Bi\{Fe(CO)_4\}_2]^-$	216.6
$[Ph_2Bi\{Cr(CO)_5\}\{Fe(CO)_4\}]^-$	226.4, 221.0, 217.2

Table 9. Selected Angles (deg) for Other Representative Organobismuth Complexes

complex	C−Bi−C	C−Bi−M	ref
Ph_3Bi	96.7 ± 1.0		25
Me_3Bi	92(1), 94(1), 96(1)		26
$[Ph_2BiFe(CO)_4]^-$	94.9(6)	101.6(4), 104.0(6)	8
$(Ph_2Bi)_2Fe(CO)_4$	94.7, 97.6	100.6(3), 101.4(4)	8
$Ph_2BiMn(CO)_5$	94.5(5)	99.2(4), 103.3(3)	8
$Ph_2BiCo(CO)_3(PPh_3)$	95.7(8)	100.9, 98.5	9
$Ph_3BiCr(CO)_5$	102.6(2), 101.8(2), 103.4(2)	118.5(2), 114.6(2), 123.6(2)	5

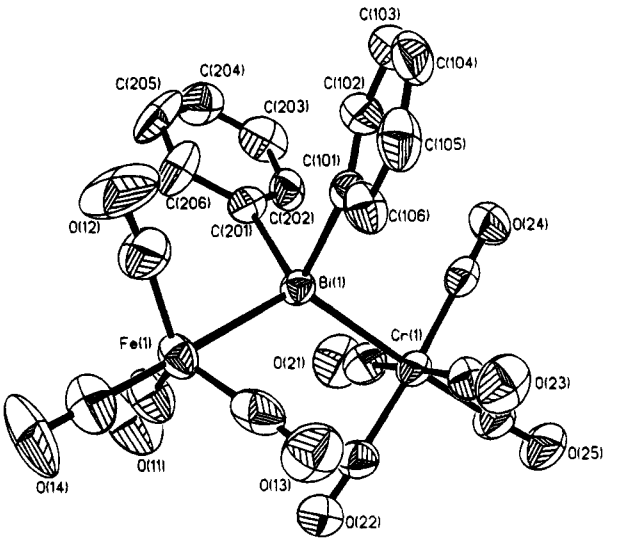

Figure 3. Diagram of the anion of [PPN][**3**]·0.48$C_4H_{10}O$ showing the displacement ellipsoids (50% probability level) and the atomic labeling scheme.

versus 2.705(1) Å for $Ph_3BiCr(CO)_5$[5]—reveals that the opposite is true. The slightly longer bond in [**1a**]$^-$ could be simply a result of steric factors; however, an alternative explanation is that the bismuth atom in [**1a**]$^-$ uses sp^3-like orbitals to form the bismuth−metal and bismuth−carbon bonds. It is well established that bond length increases as the degree of s character in the bonding orbitals decreases. This has been discussed in detail for a wide range of main group element compounds.[28]

Comparison of the bismuth−metal bond distances in the closely related clusters $[Ph_2BiFe(CO)_4]^-$ and [**2**]$^-$ further supports the postulate that the lone pair in three-coordinate bismuth clusters resides in an s-like orbital and that the longer bond seen for [**1a**]$^-$ versus $Ph_3BiCr(CO)_5$ is not simply caused by steric factors. The Bi−Fe bond in $[Ph_2BiFe(CO)_4]^-$ (2.677(4) Å),[8] is longer than those seen in [**2**]$^-$ (2.625(2) and 2.630(2) Å), where the bismuth is four-coordinate. If the longer Bi−Cr bonds in [**1a**]$^-$ are caused by steric factors, then the bond length seen in [**2**]$^-$ should likewise be *longer* than those in $[Ph_2BiFe(CO)_4]^-$. That the opposite is true indicates that steric considerations do not dominate the bonding picture. Again, the cause of the longer bond in $[Ph_2BiFe(CO)_4]^-$ can be explained on the basis of hybridization. The Bi−Fe bond in $[Ph_2BiFe(CO)_4]^-$ could contain significantly more p character than that in [**2**]$^-$ where the Bi−Fe bonds are required to incorporate the s orbital. A bond formed to an orbital having higher p character should be longer than a similar bond formed with higher s character.

The bismuth−molybdenum bonds in [**1b**]$^-$ (2.882(2) and 2.885(2) Å) are slightly longer than those observed in the recently reported mixed carbonyl−alkoxide cluster $[Et_4N]_2[BiMo_4(CO)_{12}(\mu_3\text{-}OMe)_3]$ (2.822(2) Å average),[29] but they are significantly shorter than those seen in several other bismuth−molybdenum clusters, such as $EtBi\{CpMo(CO)_3\}_2$ (2.994(1) and 2.996(1) Å),[12] $BrBi\{CpMo(CO)_3\}_2$ (2.954(2) Å),[30] $Mo_2(CO)_4(C_5H_4Me)_2(\mu\text{-}\eta^2\text{-}Bi_2)$ (2.917(2) Å),[31] $ClBi\{CpMo(CO)_2(CNtBu)\}_2$ (2.954 (2) Å),[32] and $[PPN][BiCl_2\{CpMo(CO)_3\}]$ (2.988(3) Å).[33] The shorter Bi−Mo bonds seen in [**1b**]$^-$ in relation to most of the compounds reported in the literature may

(28) Bent, H. A., *Chem. Rev.* **1961**, *61*, 275.

(29) Shieh, M.; Mia, F.-D.; Peng, S.-M.; Lee, G.-H. *Inorg. Chem.* **1993**, *32*, 2785.

(30) Clegg, W.; Compton, N. A.; Errington , R. J.; Fisher, G. A.; Hockless, D. C. R.; Norman, N. C.; Williams, N. A. L.; Stratford, S. E.; Nichols, S. J.; Jarret, P. S.; Orpen, A. G. *J. Chem. Soc., Dalton Trans.* **1992**, 193.

(31) Clegg, W.; Compton, N. A.; Errington, R. J.; Norman, N. C. *Polyhedron* **1988**, *7*, 2239.

(32) Clegg, W.; Compton, N. A.; Errington, R. J.; Norman, N. C.; Tucker, A. J. *J. Chem. Soc., Dalton Trans.* **1988**, 2941.

result from the smaller steric demand of carbonyl ligands in comparison with the cyclopentadienyl ligand.

A reviewer has suggested that the shorter bond distances in $[\mathbf{1b}]^-$ could be attributed to differences in oxidation state at bismuth, with higher oxidation states giving rise to shorter bonds. The bismuth ion in $[\mathbf{1b}]^-$ can be viewed formally as being 5+ while the other examples given have Bi in the 3+ oxidation state. This may also explain the short Bi−Mn bond distances in $[\{Cp(CO)_2Mn\}_2BiCl]_2$, which has been described as a Bi(I) compound although Bi(V) is also a possibility. The short Mn−Bi bond distances were attributed to multiple bonding. Bi(V) should have a significantly smaller radius than Bi(III), and alternatively, this could explain the short distances. Simple electron distribution rules allow assignment of a structure obeying the 18-electron rule at Mn and the octet rule at Bi without the need of invoking multiple bonding. This simplistic picture has Bi donating electron pairs to both Mn centers to which it is bonded and forming a covalent linkage to Cl. The octet at Bi is completed by acceptance of two electrons from a Cl of an adjacent $\{Cp(CO)_2Mn\}_2BiCl$ fragment, resulting in the observed dimer formation.

While these oxidation state arguments have appeal, they should be advanced with caution, as the "real" oxidation states may be quite different from those formally derived. The chemistry of these species is, for example, more consistent with that expected for low-valent bismuth centers that for Bi(V). It is also counterintuitive that highly oxidizing Bi(V) would be directly attached to highly reducing metal carbonyl anions without some electron exchange process occurring to help equalize the potential differences.

Bonding in the isoelectronic complex$[\{Cp(CO)_2Fe\}_2InCl]_2$ was recently discussed.[34] Another possible source of bond shortening was postulated to arise via π-overlap between Fe d orbitals and the In−Cl σ^* system.

The bond angles in $[\{Cp(CO)_2Mn\}_2BiCl]_2$ show the same trends as in $[\mathbf{1}]^-$, $[\mathbf{2}]^-$, and $[\mathbf{3}]^-$, but the Mn−Bi−Mn angle is much larger (141.0(2)°) and the Cl−Bi−Cl angle is much smaller (76.7(2)°), which is consistent with the hybridization distributions developed by Bent.[28] In a four-coordinate compound with two different types of substituents, it was noted that the orbitals will tend to deviate from pure sp^3 hybridization, with the more electronegative substituents inducing a higher p character into the orbitals to which they are bonded. Thus in $[\{Cp(CO)_2Mn\}_2BiCl]_2$ the Cl ligands are more electronegative than the $Cp(CO)_2Mn$ groups, which leads to the Bi−Mn bonds having a higher degree of s character and a larger Mn−Bi−Mn angle. Similar arguments can be made for $[\mathbf{1}]^-$, $[\mathbf{2}]^-$, and $[\mathbf{3}]^-$ where Ph would be a more electronegative group than the metal carbonylate fragments. Here the C−Bi−C angles fall in the range 94−96° while the M−Bi−M angles lie between 121 and 127°. The role that the electronegativity differences plays in determining the hybridization (and thus the bond angles) is obscured by the steric demands of the bulky ML_n groups. Thus the extremely large angle in $[\{Cp(CO)_2Mn\}_2BiCl]_2$ may also in part result from the smaller size of Cl versus Ph, which would allow the $Cp(CO)_2Mn$ fragments to move farther apart.

The bismuth−tungsten bonds in $[\mathbf{1c}]^-$ (2.891(2) and 2.887(3) Å) are similar to those seen for $[W_2(CO)_8(\mu\text{-}\eta^2\text{-}Bi_2)(\mu\text{-}BiMeW(CO)_5]$ between the organobismuth fragment and the $W_2(CO)_8$ unit of the cluster, 2.881(1) and 2.864(1) Å.[14] However, the bond between the bismuth and the external $W(CO)_5$ fragment is slightly shorter (2.851(1) Å) than those observed for $[\mathbf{1c}]^-$. If the bond between $W(CO)_5$ and the bismuth atom is considered a donor bond rather than a covalent bond, then this difference is consistent with the bond lengths seen in the chromium and iron clusters discussed above. The Bi−W bonds between the Bi_2 and the $W_2(CO)_8$ fragments (average 2.994(6) Å) and those observed in $Bi_2\{\mu\text{-}W(CO)_5\}_3$ (3.11(2) Å average)[35] are significantly longer than those found in $[\mathbf{1c}]^-$.

The Bi−C distances in $[\mathbf{1}]^-$, $[\mathbf{2}]^-$, and $[\mathbf{3}]^-$ range from 2.20(3) to 2.30(1) Å and average 2.25(3) Å. These distances compare well with those of the other structurally characterized metalated arylbismuth complexes such as 2.27(2) and 2.32(1) Å in $[Ph_2BiFe(CO)_4]^-$, 2.24(1) Å (average) in $(Ph_2Bi)_2Fe(CO)_4$, 2.25(1) Å in $[PhBiFe(CO)_4]_2$, and 2.23(1) and 2.27(1) Å in $Ph_2BiMn(CO)_5$,[8] as well as those found in Ph_4Bi_2, 2.28(2) and 2.26(2) Å.[8,36]

Preliminary electrochemical studies indicate that the clusters $[\mathbf{1}]^-$ can all be irreversibly oxidized under reasonably mild conditions. On the basis of this finding, the chemical oxidation of these clusters with multiple oxidants was investigated. It was hoped that a one-electron oxidation would lead to cleavage of an aryl−bismuth bond. Rupture of this bond should produce a highly reactive species, which would likely undergo aggregation processes resulting in higher nuclearity species. Unfortunately, even under fairly mild conditions, such as the addition of Cu^+ at room temperature, the outcome has been complete degradation of the metal framework. The only identifiable products are $M(CO)_5(MeCN)$ (M = Cr, Mo, W) along with small amounts of triphenylbismuth and benzene. An insoluble gray metallic precipitate, which is most likely elemental bismuth, is also produced. The oxidation process was also investigated by low-temperature ^1H NMR spectroscopy using triflic acid as the oxidant. Addition of the acid produced no signals which could be attributed to a metal hydride. It is unlikely that any signal would be observed for a bismuth-bound hydrogen because of the quadrupolar nature of bismuth ($I = {}^9/_2$). However, the formation of Ph_3Bi does imply the intermediacy of an organobismuth species, with the most likely candidate being Ph_2BiH. Diphenylbismuthine is reported to decompose above −40 °C. Furthermore, it is well-known that organobismuth compounds undergo redistribution of their organic fragments quite rapidly. Therefore the production of both metallic bismuth and Ph_3Bi can be rationalized by the following process:

$$3Ph_2BiH \rightarrow 2Ph_3Bi + BiH_3$$

$$BiH_3 \rightarrow Bi + {}^3/_2H_2$$

As mentioned earlier, the lone pair on the bismuth of $[Ph_2BiFe(CO)_4]^-$ was thought to be inert to electrophiles because of the product isolated when it was allowed to react with Ph_2BiCl was $(Ph_2Bi)_2Fe(CO)_4$ rather than a dibismuthine derivative.[8] In contrast to this result, the reaction of $[Ph_2BiFe(CO)_4]^-$ with unsaturated transition metal fragments leads to metalation at bismuth. These new results suggest that a different explanation can be put forth to explain the product seen in the reaction of $[Ph_2BiFe(CO)_4]^-$ with Ph_2BiCl (Scheme 1).

Like its lighter analogs, $[Ph_2BiFe(CO)_4]^-$ could attack the Ph_2BiCl at the bismuth atom instead of from the iron atom as had been previously postulated.[8] This approach would generate

(33) Clegg, W.; Compton, N. A.; Errington, R. J.; Fisher, G. A.; Hockless, D. C. R.; Norman, N. C. *Polyhedron* **1991**, *10*, 123.
(34) Clarkson, L. M.; Norman, N. C.; Farrugia, L. J. *Organometallics* **1991**, *10*, 1286.
(35) Huttner, G.; Weber, U.; Zsolnai, L. *Z. Naturforsch.* **1982**, *37B*, 707.
(36) (a) Calderazzo, F.; Morvillo, A.; Pelizzi, G.; Poli, R. *J. Chem. Soc., Chem. Commun.* **1983**, 507. (b) Calderazzo, F.; Poli, R.; Pelizzi, G. *J. Chem. Soc., Dalton Trans.* **1984**, 2365.

Scheme 1. Proposed Mechanism for the Formation of $(Ph_2Bi)_2Fe(CO)_4$

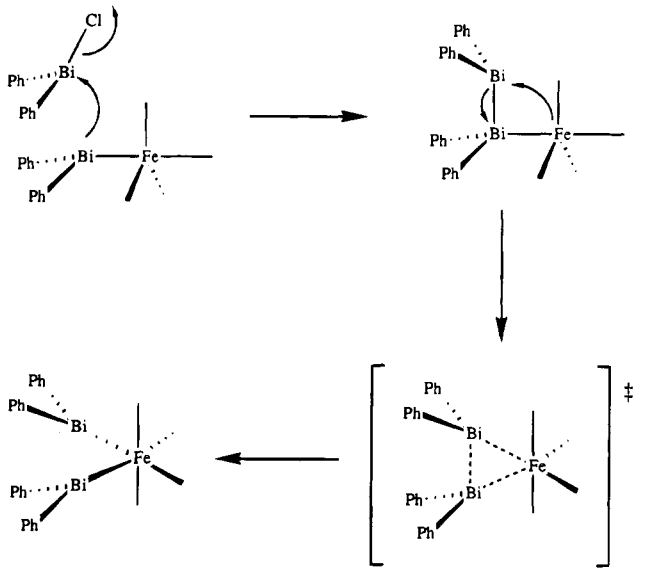

an $Fe(CO)_4$-substituted dibismuthine. Compounds which are isostructural with this have been isolated for the lighter group 15 elements phosphorus and arsenic[37] via this synthetic route. However, the E_2R_4 compounds (E = P, As, Sb, Bi) become progressively less stable as E gets larger. This decreasing stability would promote a 1,2 migration of the diphenylbismuth moiety onto the iron atom, generating the observed product, $(Ph_2Bi)_2Fe(CO)_4$. Interestingly, the transition state for this migration should be virtually identical to the intermediate which is thought to occur in the reaction of Ph_4Bi_2 with reactive fragments such as $Fe(CO)_4$ or $:CH_2$.[8,38]

Conclusion

Reaction of Ph_2BiCl with transition metal carbonylates produces mixed organo−metal−bismuth complexes in high yield. When dinuclear carbonylate anions such as $[M_2(CO)_{10}]^{2-}$ are used, the product contains a tetrahedral bismuth center in which the lone pair, which was formerly thought to be chemically inert, binds a second metal fragment. This approach is also successful with other dinuclear anions such as $[Fe_2(CO)_8]^{2-}$. Alternatively, these tetrahedral clusters can be produced by allowing the monometalated complex $[Ph_2Bi\text{-}Fe(CO)_4]^-$ to react with unsaturated transition metal fragments. These results indicate that the lone pair on bismuth in these mixed species can be basic and nucleophilic under appropriate conditions. Both the structural and reactivity patterns observed in this study indicate that it is more appropriate to view the lone pair on bismuth as "plastic" rather than "inert". When the lone pair is needed for bonding, the hybridization at bismuth readily becomes sp^3-like, while when the lone pair is not needed for bonding, it retreats into an s-like orbital and the remaining bonding orbitals take on a corresponding p-like character.

Acknowledgment. K.H.W. wishes to thank the National Science Foundation and the Robert A. Welch Foundation for financial support of this work and for assistance in the purchase of the X-ray diffractometer. R.E.B. wishes to thank the NSF for a Predoctoral Fellowship. VG Analytical and Finnigan MAT are acknowledged for providing the FABMS analyses.

Supplementary Material Available: Full tables of the interatomic bond distances and angles and the positional and anisotropic displacement parameters for [PPN][**1a−c**], [Et_4N][**2**], [PPN][**3**], and **4** and diagrams of the anions of [PPN][**1b**] and [PPN][**1c**] as well as the two independent molecules of **4** (71 pages). Ordering information is given on any current masthead page.

IC940691Y

(37) Collman, J. P.; Komot, R. G.; Siegl, W. O. *J. Am. Chem. Soc.* **1973**, *95*, 2389.
(38) Steinseifer, F.; Kauffman, T. *Angew. Chem., Int. Ed. Engl.* **1980**, *19*, 723.